SpaceOps-2021,7,x1504

Attitude control of the disposal phase of the eCube mission for atmospheric data acquisition

Francesca Scala[a], Mirko Trisolini[b], Camilla Colombo[c]*

[a] *Department of Aerospace Science and Technology, Politecnico di Milano, Via La Masa, 34, 20156 Milano - Italy*, francesca1.scala@polimi.it

[b] *Department of Aerospace Science and Technology, Politecnico di Milano, Via La Masa, 34, 20156 Milano - Italy*, mirko.trisolini@polimi.it

[c] *Department of Aerospace Science and Technology, Politecnico di Milano, Via La Masa, 34, 20156 Milano - Italy*, camilla.colombo@polimi.it

* Corresponding Author

Abstract

This paper aims at providing a new perspective on the attitude dynamics and control system of a new CubeSat mission concept for atmospheric data acquisition, in the region between 200 km and 100 km, for more accurate re-entry predictions. It discusses the main challenges and the feasibility of analysing the main atmospheric parameters via onboard sensors of a 12-unit CubeSat, designed at Politecnico di Milano. The paper presents the attitude control system feasibility during the data-acquisition phase, when the disturbance given by the atmospheric density is highly affecting the CubeSat dynamics, before the atmospheric disposal. After the estimation of the maximum momentum storage and the maximum torque acting on the satellites, a control law is provided to control the attitude via reaction wheels, allowing the data acquisition from the onboard sensors. Moreover, an analysis of the desaturation strategy is presented, to satisfy the pointing accuracy for the measurements of the network of sensors. The analysis could provide a baseline for future similar mission in the same orbital region, to enhance the acquisition of atmospheric data.

Keywords: thermosphere characterization, attitude control, CubeSat mission

1. Introduction

In the context of the European Space Situational Awareness (SSA) and Space Traffic Management (STM), Politecnico di Milano is developing a CubeSat mission concept, the environmental CubeSat (e.Cube), which will contribute to the development of key areas to ensure a safer and more sustainable access to Space [1]. In the rapidly evolving scenario of New Space activities, large constellations, and the increasing dependence of our daily life on Space, the European Space Agency (ESA) has identified the mitigation of space debris as one of the main goals for sustainable development of space activities in the near future. The mission wants to revolutionise the current state-of-the-art knowledge of the Low Earth Orbit environment, developing and validating an onboard algorithm for autonomous collision avoidance, characterising the untraceable space debris object to improve the debris environmental models and the upper atmosphere for more accurate re-entry prediction. The mission concept has been carried out at Politecnico di Milano, in collaboration with D-Orbit for the CubeSat platform design, Intelligentia for the onboard software implementation, Università di Padova for the debris detection payload, and TEMIS for the atmosphere data collector payload.

This paper focuses on the Attitude Dynamics and Control System (ADCS) design of the last phase of the mission, after an end-of-life manoeuvre for the re-entry. During the re-entry phase, an experiment through an atmospheric data collector will characterise the thermosphere in the region below 200 km, through some in-situ measurements, in particular density, temperature, and pressure. The data and results of the e.Cube mission will be used to validate tools and techniques currently used by the space debris community for improving and validating re-entry predictions.

In this framework of sustainable use of space, one of the key aspects to ensure future accessibility is the implementation of mitigations measures. The prediction of the re-entry evolution and trajectory is difficult and one of the main sources of uncertainty is the atmospheric density, which greatly influences the decay time of the satellite. The disposal of spent satellites through a re-entry within 25 years of their decommissioning is one of the main strategies. However, during the re-entry of a satellite, the safety of people and properties on the ground must be ensured by limiting the probability that surviving fragments will land in populated areas. On one hand, the prediction of the re-entry evolution and trajectory is difficult and one of the main sources of uncertainty is the atmospheric density, which greatly influences the decay time of the satellite. Density estimates have been obtained via accelerometer data gathered by missions such as GRACE, CHAMP, and TerraSAR-X [2]. On the other hand, understanding the destructive re-entry process is crucial for casualty risk predictions [3][4][5]. Re-entries have been analysed indirectly, via observation through ground optical instruments. The data collected have been used to improve atmospheric and breakup models. Airborne observations have been carried out for a few missions, such as the re-entry of the European Automated Transfer Vehicle (ATV) Joule Verne [3] in 2008, and of the Hayabusa sample-return capsule in 2010 [4]. Ground and airborne observations have limitations due to the harsh re-entry environment that is characterised by ionisation and dissociation phenomena, which reduce observation capabilities. These types of observations cannot give information on the loads experienced by the spacecraft. A different approach has been implemented by the Aerospace Corporation, which has developed the Re-entry Breakup Recorder (REBR). The device records temperature, acceleration, rotational rate, GPS during the re-entry. REBR is designed to survive the re-entry environment and transmit the gather data before impacting the ground [5]. The most recent mission, in 2019, is the QARMAN CubeSat mission, led and built by Von Karman Institute (VKI), for ESA. The objective of the mission is to demonstrate re-entry technologies, new passive aerodynamic drag and attitude stabilization systems, and the transmission of telemetry data during re-entry via data relay satellites in LEO [6].

Improving the accuracy of re-entry predictions and the understanding of the break-up phenomenon is of great importance to ensure the safe disposal of decommissioned satellites. Given that the uncertainty in re-entry prediction is dominated by the uncertainty in the atmospheric density, the e.Cube mission wants to provide direct measurements of the in-situ atmospheric pressure, temperature, and density to contribute to the current modelling of the atmosphere. At the same time, the objective of the e.Cube mission is to improve the knowledge of the mechanisms behind the destructive phase by gathering first-hand measurements during this process in the latest stage of the re-entry phase. For this purpose, it will mount a re-entry data collector to improve the current re-entry prediction models and the knowledge of thermomechanical loads experienced by the spacecraft. The payload includes a triaxial accelerometer, pressure sensors, heat flux sensors and an inertial measurements unit. This network of sensors measuring the internal temperature, pressure, vibrations, and displacements of the spacecraft parts will be used to monitor the behaviour of the spacecraft.

This work presents the design of the ADCS during the atmospheric re-entry of the e.Cube mission. The objective of the analysis is to provide stable attitude control for the CubeSat to allow the characterisation of atmospheric properties. The feasibility of a control system based on commercial-off-the-shelf components is evaluated to reduce the time and cost of the mission. The onboard distributed sensors for the atmospheric measurements require a three-axis stabilised attitude control of the CubeSat. Moreover, during the re-entry analysis experiment, the system should maintain a data relay connection to download the acquired data. A simulation algorithm is proposed in the Matlab/Simulink® environment to assess the feasibility of the ADCS system. The CubeSat is considered subject to external orbital perturbations, such as the atmospheric drag, the solar radiation pressure, and the gravitational perturbations. A preliminary selection of the onboard sensors and actuator is presented. To ensure a correct attitude of the CubeSat during the mission lifetime, the system is controlled on the three axes with reaction wheels (RW). The desaturation control of the RWs is performed using together magneto torquers. The need for introducing CubeSat thruster modules is evaluated, relying on cold-gas thrusters. The selection of the actuators is driven by the requirements related to the operational phase during the atmosphere analysis.

2. eCube mission concept overview

The eCube is a mission concept composed of one 12U CubeSat satellite, that will fly in Low Earth Orbit (LEO) to provide data and analysis on the LEO environment, as well as on the thermosphere characterisation. More specifically, e.Cube tackles three main scientific objectives:

- Development, validation, and testing of onboard algorithms for autonomous collision avoidance.
- Characterisation of untraceable space debris objects to update and improve space debris environmental models.
- Characterisation of the upper atmosphere for more accurate re-entry prediction and of the thermomechanical loads experienced by the spacecraft during re-entry.

These objectives address distinct but interlinked aspects of space sustainability, spanning the entire lifetime of any space mission. The first two objectives investigate the two sides of the same spectrum: the collision avoidance of traceable debris on one side and the improvement of the damage assessment from untraceable debris on the other. Starting from the scientific objectives, the CubeSat platform has been designed to respect the scientific and mission requirements of the mission. The CubeSat platform size was driven both by the dimensions of the scientific payload instrument and by the need to mount onboard a propulsive system. A preliminary analysis of the scientific payloads highlights the need of reserving at least 1-unit each to the debris detection instrument, the collision avoidance payload, and the atmospheric data detector. Moreover, the propulsive system could occupy from 1 to 2 unit of the satellite. Consequently, the 12-unit module has been selected, leaving 9-unit for the development of the service module, two of them occupied by the propulsive system.

2.1.1 Scientific requirement description

The main scientific objectives of the e.Cube mission are summarised in Table 1 [1]. The accuracy requirements are key parameters for the design of the ADCS subsystem it will ensure correct data collection in every phase of the mission. During the space debris particle detection phase, the instrument shall continuously point the velocity direction to maximise the number of impacts of sub-millimetre debris particle. Moreover, during the thermosphere data detection phase, where it is important to maintain a stable attitude in the velocity pointing to provide correct measurements of temperature and pressure of the upper part of the atmosphere. The requirement on the maximum slew rate admissible not only impacts the stability of the data collection and the data accuracy but also poses a constraint in the collision avoidance manoeuvre design.

Table 1: e.Cube scientific requirement for orbital and attitude control design.

Description	Value
Resolution of the debris particle detection instrument	1 μm – 1 mm
Resolution of temperature and pressure of the thermosphere	10 km
Pointing accuracy during the debris particle detection phase	1 deg
Maximum slew rate	1 deg/s
Pointing accuracy during the thermosphere data analysis phase	5 deg

Starting from the need to maximising the number of submillimetre particle impact on the detection instrument together with the requirements for the LEO protected region, the adopted reference orbit for debris environment characterisation is a Sun Synchronous Orbit at about 550 km of altitude. Moreover, during the final part of the mission, dedicated to the atmospheric analysis, the CubeSat will be manoeuvred on an elliptical orbit with the perigee below 200 km. In this way, the spacecraft will analyse at every passage the thermosphere properties, such as temperature,

pressure, and atmospheric density. For this purpose, an orbit with dimensions 550 x 180 km is selected, to provide a slow decay of the satellite in the region between 200 km and 100 km, before the final atmospheric re-entry. The parameters of these orbits are described in Table 2. The preliminary analysis using the MASTER® tool shown a resulting permanence time of few weeks in the interesting region. Such permanence time allows the characterisation of the thermosphere properties at each perigee passage, with multiple possibilities to transmit the data on-ground before the mission disposal. During this phase, the high perturbation level of this region, due to the drag effect, poses a challenge in the design and simulation of the attitude dynamics and control (ADCS) system of the CubeSat.

Table 2: e.Cube reference orbit during re-entry phase

Parameter	Symbol	Value
Perigee altitude	h_p	180 km
Apogee altitude	h_a	550 km
Inclination	i	96.90°
Eccentricity	e	0.0274

2.1.2 Platform requirement description

The scientific requirements influence the design of the platform and, particularly, of each subsystem. The most important requirements are reported in Table 3, where requirements for the propulsion, power and telecommunication subsystem are shown. The accuracy requirements for the ADCS subsystem are the value reported in Table 1 [1].

Table 3: e.Cube platform requirements

Description	Value
Delta-v budget for collision avoidance and re-entry manoeuvres	125 m/s
Maximum thrust level	500 mN
Average and peak power budget during the debris analysis phase	22 W // 29 W
Average and peak power budget during collision avoidance phase	17 W // 53 W
Average and peak power budget during re-entry analysis phase	18 W // 25 W
Data rates	600 kB/day

The preliminary e.Cube external configuration is depicted in Fig. 1. The front view is shown in Fig. 1 (left), where the debris detection instrument is visible in the front 4-unit surface. Moreover, deployable solar panels are considered to provide the correct power generation for the system. Fig. 1 (right) shows the back view of the external configuration, where it is possible to identify the antennas systems and the onboard engine. Two S-band antennas are mounted to transmit the scientific data of the payloads, moreover, a GPS antenna is employed for the reconstruction of the satellite state during the mission. The thrusters have been mounted on the opposite side of the debris detection instrument, to minimise the interference and the degradation effect of the plume. Finally, some solar panels are mounted in the back part of the satellite to provide power generation for different orbital configuration of the CubeSat.

The preliminary spacecraft mass budget is about 15 kg (considering a 20% margin for this preliminary mission assessment), where the most demanding subsystems are the ADCS and the propulsion components covering about 2.5 kg and 3.4 kg, respectively. The payload components account for about 3 kg altogether [1].

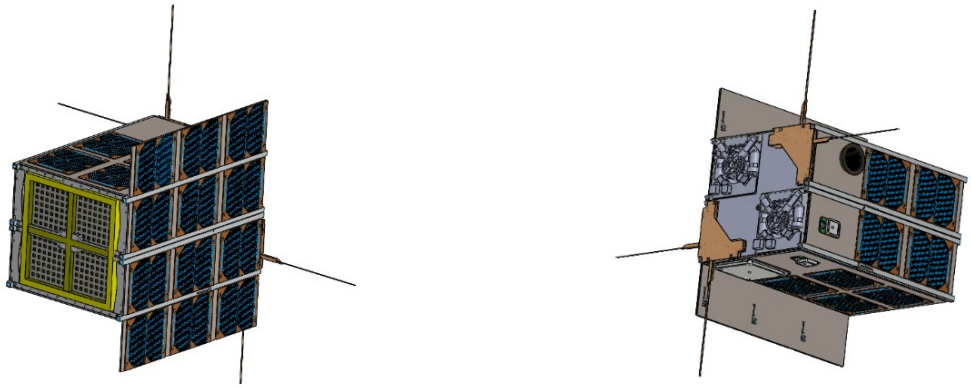

Fig. 1: Preliminary configuration of the e.Cube spacecraft: front view (left), back view (right).

3. Atmosphere Analysis and Disposal Scenario

The final part of the e.Cube mission operations aim at characterising the re-entry of the spacecraft, thus, it is vital to design a proper disposal scenario. As the disposal phase is also part of the operational phase of the mission, it must be carried out within a timeframe that is compatible with the lifetime and reliability of CubeSat components. Therefore, a maximum disposal time of 6 months has been considered. The CubeSat will perform disposal manoeuvres to lower its perigee altitude and ensure compliance with this requirement [1].

Another important aspect is the time spent in the lower parts of the atmosphere to maximise the acquisition of relevant data during the re-entry. For this purpose, a Re-entry Data Collector (RDC) payload will include a triaxial accelerometer which, together with the pressure, the temperature, and the density, will give the possibility to estimate the thermomechanical loads. The implementation of the Re-entry Analysis Phase is based on the maximisation of the time spent below an altitude of 200 km to enhance the data collection. A strategy to lower the perigee could be beneficial to the Re-entry Analysis Phase, increasing the residence time below 200 km of altitude and ensuring multiple passages in such region during the decay period. The apogee and perigee decay evolution for the 550 x 180 km orbit is shown in Fig. 2. The strategy proposed allows the perigee to remain more than 30 days in the region of interest under 200 km. In this scenario, the estimated decay time is about 42 days and the overall time spent below 200 km is about 7 days and 23 hours.

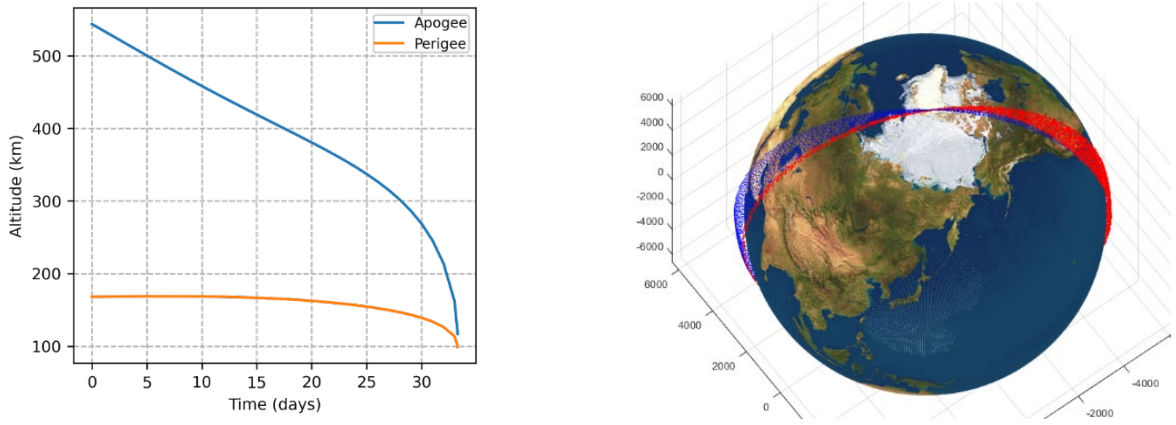

Fig. 2: Apogee and perigee decay evolution for a 550 x 180 km orbit (left). Evolution of the orbit with in red the portion spent under 200 km (right).

The Re-entry Data Collector has two main objectives: the measurements of the atmospheric density, below 200 km, and of the thermomechanical loads during the final mission phase before the atmospheric break-up. The physical properties required for the instrument composing the RDC are reported in Table 4.

First, the knowledge of the air density in the thermosphere is crucial for improving the accuracy of the SW models used to estimate the re-entry trajectory of debris. A first approach is identified in the direct measurement of the density in situ, which was typically performed with expensive payloads, not suitable for a CubeSat mission. Nevertheless, a second indirect approach can be considered: the density can be computed also as an indirect parameter after the measurement of other quantities, in particular temperature and pressure. The latter approach is suitable for CubeSat mission, being the temperature and pressure sensors for CubeSat already available on the market, and they do not need any development or customisations. The second objective of the RDC is the understanding of the thermal and mechanical loads acting on the CubeSat during the latest phase of its life. Inertial Measurement Units (IMUs) based on Micro-Electro-Mechanical Systems (MEMS) technology are the state-of-the-art and several Commercial off-the-shelf (COTS) options are currently available on the market. The inclusion of temperature sensors and strain gauges to measure the internal heat loads and displacements, respectively, will be considered in Phase A, when a more consolidated internal design of the CubeSat will be available.

Table 4: Physical properties of the Re-entry Data Collector payload.

Description	Measurements ranges
Pressure sensors	10^{-3} to 10^{5} Pa
Heat flux sensors	-200 to 150°C
Inertial measurements units	$\pm$ 5 g

4. Model of the Attitude Dynamic and Control System

The AOCS is a fundamental subsystem for the success of the mission. During the re-entry analysis experiment, the system shall be able not only to maintain a data relay connection to download the acquired data until an altitude of 100 km but also to maintain the CubeSat pointing the velocity direction for stable and accurate data collection. This section focus on the model of the attitude dynamics and control system of the e.Cube mission. To ensure a correct attitude of the CubeSat during the mission lifetime, the system is controlled on the three axes with reaction wheels (RWs). The desaturation control of the RWs is performed using together magneto torquers and, if needed, CubeSat attitude thruster module, relying on cold-gas thrusters, aligned with the centre of mass, thus minimizing parasitic torques (nominally null). The main requirement for the ADCS during the atmospheric analysis phase is to provide a 5 deg pointing accuracy. This requirement is driven by the onboard sensors, for correct data acquisition. As described in Section 2.1.2, the structure of the spacecraft is a standard 12U CubeSat, which is compatible with the integration of COTS components. During phase A of the mission, possible customization to the standard 12U structure will be evaluated.

4.1 Actuators and sensors of the ADCS

As a preliminary analysis, the actuators and the sensors for the ADCS are selected from the COTS components. Table 5 shows the preliminary components selection for the analyses presented in this paper. The components are selected among the flight proven CubeSat components, currently available on the market. Given the currently available sensors for CubeSats, the expected accuracy of the attitude determination system is up to 0.05 degrees when star-trackers are included. The cold gas module could be included in the architecture for reaction wheels desaturation purposes.

Table 5: Preliminary actuators and sensors selection for the ADCS of the e.Cube [7][8][9][10][11].

Description	Supplier	Main properties	Value
Reaction Wheels	Hyperion technologies	Maximum momentum storage	50 mNms
		Maximum torque	12 mNm
Magnetorquers	New Space System	Maximum torque	1.19 Am^2
Cold Gas Module*	MicroSpace Srl	Maximum thrust	10 mN
Sun sensors	GOM space	Accuracy (3-sigma)	0.017 deg
Magnetometer	GOM space	Accuracy (3-sigma)	0.5 deg
Star tracker	OCE Technology	Accuracy (3-sigma)	10 arcsec

* optional component

4.2 Architecture of ADCS subsystem

The block scheme architecture of the ADCS subsystem of e.Cube is shown in Fig. 3. The Euler equations and the quaternion kinematics are used to describe the CubeSat attitude dynamics, subject to external perturbations. The model includes the effect of the Earth gravity potential, the magnetic disturbance, the drag perturbation, and the solar radiation pressure effect (including the eclipse periods). For the attitude reconstruction, three sensors are modelled, the sun sensors, the star trackers and the magnetometer. A Davenport's q-method determination algorithm is implemented for attitude reconstruction [12]. At this point, the error with respect to the reference attitude is computed. For the analysis case, the reference attitude is velocity vector pointing to provide a stable configuration for pressure and temperature measurements. Finally, a Direction Cosine Matrix proportional control is implemented to provide the commanded control for the tetrahedral reaction wheels assembly [13]. The magneto torquers are continuously used to provide a desaturation component. The thrusters are included to balance the difference between the desaturation torque required and the magnetometer torque.

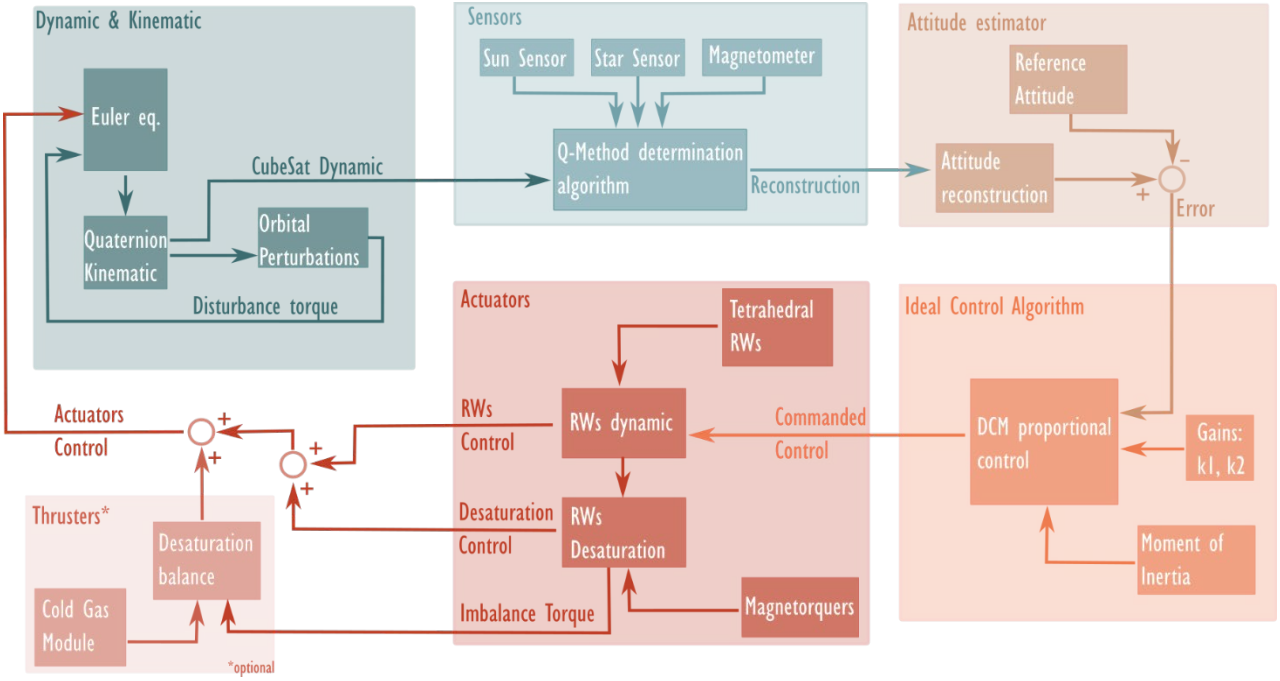

Fig. 3: Block diagram of the ADCS architecture for e.Cube spacecraft.

4.3 Attitude determination

A spacecraft attitude determination system typically uses a combination of sensors and mathematical models to collect vector components in the body and inertial reference frames. Since attitude is described by three or more attitude variables, the difference between the desired and measured states can be subjected to some reconstruction errors, described by the determination error:

$$e_{det} = \text{trace}\left(\boldsymbol{I} - \boldsymbol{A_B^{sens}} \cdot (\boldsymbol{A_B^{mod}})'\right) \tag{1}$$

Where $\boldsymbol{A_B^{sens}}$ is the attitude in the body frame computed by the onboard sensors, and $\boldsymbol{A_B^{mod}}$ is the attitude in the body frame computed from the numerical models. The reconstruction error e_{det} should be smaller than the unit to grant a precise sensor measurement, coherent with the model determination matrix $\boldsymbol{A_B^{mod}}$.

An elegant way of solving the attitude determination problem is the q-Method [12]. It is based on the minimization of a cost function $J\ (\boldsymbol{A_B})$. It is typically more accurate than other methods as the TRIAD algorithm [14]. The q-Method reduces the minimization process of the cost function to an eigenvalue problem, where the optimal attitude estimate corresponds to the eigenvector associated with the optimal eigenvalue [11].

$$J(\boldsymbol{A_B}) = \frac{1}{2} \sum_{k=1}^{N_{sensor}} \alpha_i \,||\, \mathbf{v_{Bi}} - \boldsymbol{A_B}\mathbf{v_{Ni}} \,||^2 \tag{2}$$

Where N_{sensor} is the number of sensors used for the attitude determination, and the contribution of each sensor is weighted by the α_i coefficients, chosen based on the accuracy of each instrument. The vectors $\mathbf{v_{Bi}}$ and $\mathbf{v_{Ni}}$ are the measurement provided by the sensors in the body and inertial frame respectively. The sun sensor gives the direction of the Sun, the star tracker provides the angle with the reference star, and the magnetometer provides the geomagnetic field. Starting from the optimisation problem in quaternion form, the optimal solution is given by the following eigenvalue problem [12].

$$\boldsymbol{K} = \begin{bmatrix} S - \sigma I & Z \\ Z' & \sigma \end{bmatrix} \qquad \begin{aligned} B &= \sum_{k=1}^{N_{sensor}} \alpha_i \,(\mathbf{v_{Bi}}\mathbf{v'_{Ni}}) \\ S &= B + B' \\ Z &= [B_{23} - B_{32} \quad B_{31} - B_{13} \quad B_{12} - B_{21}]' \\ \sigma &= \text{trace}(B) \end{aligned} \tag{3}$$

The largest eigenvalue and corresponding eigenvector of the matrix $\boldsymbol{K}$ are the solutions of the attitude determination problem. This is used to characterise the attitude matrix $\boldsymbol{A_B}$ reconstructed by the sensors, which minimizes the cost function in Eq. (7). The reconstruction error is shown in Fig. 5, where the determination error for our mission study case is below 10^{-5}, resulting in a precise attitude determination.

4.4 Attitude control

The problem of tracking a time-varying reference frame is considered in this section. Particularly, we developed a three-axis attitude control with a redundant set of reaction wheels. We also considered the desaturation problem in the control law, to provide continuous control of the reaction wheels during the tracking phase.

We defined $\boldsymbol{B}$ the body frame referred to an inertial frame $\boldsymbol{N}$. The inertial frame is the Earth Centred Inertial reference frame (ECI). The attitude control aims to orient the body frame $\boldsymbol{B}$ with a reference tracking frame, called $\boldsymbol{L}$, so that the spacecraft continuously tracks the reference attitude.

The spacecraft attitude dynamics in the body frame is described by the Euler equations, referred to the principal axis x, y, z of the body frame, under the effect of external disturbance $\boldsymbol{D}$, and the control moment $\boldsymbol{M}$. The body

reference frame is defined by the principal inertial axis of the orbiting body, such that the principal moment of inertia matrix $\boldsymbol{\mathcal{J}}$ and the angular velocity vector $\boldsymbol{\omega_B}$ are in the principal reference axis [15].

$$\begin{cases} \dot{\omega}_x = \dfrac{I_y - I_z}{I_x}\omega_y\omega_z + \dfrac{D_x}{I_x} + \dfrac{M_x}{I_x} \\ \dot{\omega}_y = \dfrac{I_z - I_x}{I_y}\omega_x\omega_z + \dfrac{D_y}{I_y} + \dfrac{M_y}{I_y} \\ \dot{\omega}_z = \dfrac{I_x - I_y}{I_z}\omega_y\omega_x + \dfrac{D_z}{I_z} + \dfrac{M_z}{I_z} \end{cases} \tag{4}$$

where the matrix $\boldsymbol{\mathcal{J}}$ is a diagonal matrix with the principal moment of inertia on the diagonal: I_x, I_y, I_z, and the components of the angular velocity are $\boldsymbol{\omega_B} = [\omega_x \quad \omega_y \quad \omega_z]'$. In this work, the kinematic representation has been done using the quaternions representation, since it does not inherit geometrical singularity and it is highly computationally efficient. The kinematic representation in quaternion coordinates is the following [15]:

$$\begin{bmatrix} \dot{q}_1 \\ \dot{q}_2 \\ \dot{q}_3 \\ \dot{q}_4 \end{bmatrix} = \frac{1}{2}\begin{bmatrix} 0 & \omega_z & -\omega_y & \omega_x \\ -\omega_z & 0 & \omega_x & \omega_y \\ \omega_y & -\omega_x & 0 & \omega_z \\ -\omega_x & -\omega_y & -\omega_z & 0 \end{bmatrix}\begin{bmatrix} q_1 \\ q_2 \\ q_3 \\ q_4 \end{bmatrix} \tag{5}$$

where the components q_1, q_2, q_3 represent the orientation vector in space (eigenvector), while q_4 represents the rotation around the vector (eigen-angle).

The tracking reference frame $\boldsymbol{L}$ is oriented as the velocity vector of the CubeSat. It is defined with the origin in the centre of mass of the satellite, with the three-axis unit vector oriented as: l_1 along with the velocity component of the satellite, l_3 along with the angular momentum of the satellite orbit, and l_2 to complete the right-hand side. The attitude error between the spacecraft body frame $\boldsymbol{B}$ and the reference frame $\boldsymbol{L}$ is described using the direction cosine matrices, and the angular velocity error, as follows:

$$\begin{aligned} \boldsymbol{A_{BL}} &= \boldsymbol{A_B} \cdot \boldsymbol{A_L^T} \\ \boldsymbol{\omega_{BL}} &= \boldsymbol{\omega_B} - \boldsymbol{A_{BL}}\boldsymbol{\omega_L} \end{aligned} \tag{6}$$

where $\boldsymbol{A_B}$ and $\boldsymbol{A_L}$ represents the direction cosine matrix for the body and the tracking frame, respectively. The tracking control aims to manoeuvre the body to align the body to the reference matrix so that the error tends to zero:

$$\begin{aligned} \boldsymbol{A_{BL}} &\to \boldsymbol{I} \\ \boldsymbol{\omega_{BL}} &\to \boldsymbol{0} \end{aligned} \tag{7}$$

where the matrix $\boldsymbol{I}$ is the identity matrix. The desired control law is expressed in terms of these error matrix and angular velocity error, $\boldsymbol{A_{BL}}$ and $\boldsymbol{\omega_{BL}}$ [15]:

$$\boldsymbol{u_d} = -k_1 \cdot \boldsymbol{\mathcal{J}} \cdot \boldsymbol{\omega_{BL}} - k_2 \cdot [\boldsymbol{A_{err}}]^{\vee} \tag{8}$$

where k_1 and k_2 are control gain, and $[\boldsymbol{A_{err}}]^{\vee}$ is the skew-symmetric matrix from $\boldsymbol{A_{err}} = \boldsymbol{A'_{BL}} - \boldsymbol{A_{BL}}$. The numerical value of k_1 and k_2 are selected to provide a feasible result of the control, both in terms of control effort and converging time. The stability of the control law is assessed thanks to the Lyapunov function [ref]. The Lyapunov function $V = \frac{1}{2} < \boldsymbol{\omega_{BL}}, \boldsymbol{\mathcal{J}}\,\boldsymbol{\omega_{BL}} > + k \cdot \mathrm{trace}(\boldsymbol{I} - \boldsymbol{A_{err}})$ is used to check the stability. Differentiating V, it is possible to demonstrate that $\dot{V} \ll 0$ always, granting the asymptotic stability of the control law in time.

In this paper, we consider momentum management of the ideal control by the reaction wheels assembly. The following subsections describe the control management by a redundant reaction wheels system and the desaturation management with both magneto torquers and thrusters.

4.4.1 Attitude control with redundant reaction wheels

For the e.Cube satellite, we consider a redundant reaction wheels system, including four actuators in tetrahedral configuration, as shown in Fig. 4. This configuration can provide a high level of torque, almost double as a single reaction wheel [16]. The distribution matrix for this tetrahedron configuration depends on the orientation relative to the body frame. The tilt angle with the $x_b - y_b$ plane is defined as β and could assume a varying value, typically

selected around 20°. The distribution matrix is shown in Eq. (9), where the angle α_1 and α_2 are 30° and 60° respectively, due to geometrical configuration of the assembly.

$$\boldsymbol{A_w} = \begin{bmatrix} \cos\beta & -\cos\beta\cos\alpha_2 & -\cos\beta\cos\alpha_2 & 0 \\ 0 & \cos\beta\cos\alpha_1 & -\cos\beta\cos\alpha_1 & 0 \\ -\sin\beta & -\sin\beta & -\sin\beta & 1 \end{bmatrix} \tag{9}$$

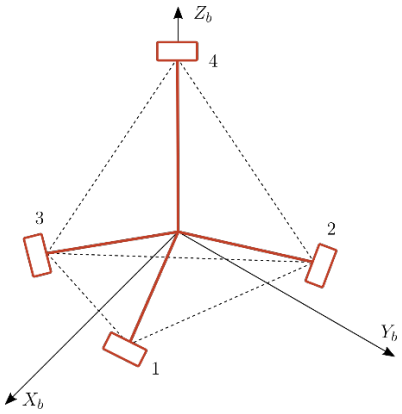

Fig. 4: Tetrahedral configuration of the reaction wheel assembly

The ideal control torque, computed in Section 4.4, is used as the commanded control for the onboard actuators. This control imposes an ideal angular momentum and torque on the actuator system, which results in a required angular velocity of the rotors. For the reaction wheel assembly, depending on the number of elements of the actuators, we define the angular momentum as $\boldsymbol{h_w} = [h_{w1},\ h_{w2},\ h_{w3}, h_{w4}]'$ and the rotation velocity of the wheel about its spin axis as $\boldsymbol{\Omega_W} = [\Omega_{w1}, \Omega_{w2}, \Omega_{w3}, \Omega_{w4}]$. The nominal condition of a RW is zero angular velocity, hence it oscillates around this condition to provide a control torque for a precise pointing manoeuvre. Its dynamic motion is actively controlled through a feedback loop. The most important characteristics of a RW are the maximum torque exerted and the momentum storage. If the torque required for the control is too high, the reaction wheel could saturate. The desaturation methodology implemented for e.Cube is discussed in Section 4.4.2.

The commanded control $\boldsymbol{u_d}$ is imposed together with the knowledge of the distribution matrix to compute the commanded control torque on the reaction wheels, $\dot{\boldsymbol{h}}_{\boldsymbol{w}}$ [15].

$$\dot{\boldsymbol{h}}_{\boldsymbol{w}} = \boldsymbol{A}_{\boldsymbol{w}}^{*} \cdot (\boldsymbol{A_w}\, \boldsymbol{h_w} \times \boldsymbol{\omega_B} - \boldsymbol{u_d}) \tag{10}$$

with $\boldsymbol{A}_{\boldsymbol{w}}^{*}$ computed from the distribution matrix as $\boldsymbol{A}_{\boldsymbol{w}}'(\boldsymbol{A_w} \cdot \boldsymbol{A}_{\boldsymbol{w}}')^{-1}$. Moreover, the wheel rotational velocity about its spin axis is computed from the knowledge of the angular momentum for each wheel i ($i = 1{:}\,4$):

$$\Omega_{wi} = \frac{h_{wi}}{\mathrm{J}_{wi}} \tag{11}$$

where J_{wi} is the wheel spin axis inertia. By integrating the Eq. (10), it is possible to recover at each time instant the angular momentum h_{wi}, the torque $\dot{h}_{wi}$ and the rotational velocity Ω_{wi} for each wheel in the assembly. These parameters are limited by the technological characteristics of the wheels; thus, a saturation limit is imposed to ensure a dynamic of the RWs in the physical ranges. The new values in the operational ranges are defined as $\widetilde{\boldsymbol{h_w}}$, $\widetilde{\dot{\boldsymbol{h}}_{\boldsymbol{w}}}$ and $\widetilde{\boldsymbol{\Omega_w}}$, depending on the physical parameters in Table 5.

Consequently, the control torque generated by reaction wheels depends on the distribution matrix and the angular momentum of the wheels and the angular velocity of the satellite $\boldsymbol{\omega_B}$ in the body frame:

$$\boldsymbol{u_w} = \boldsymbol{A_w}\, \widetilde{\boldsymbol{h_w}} \times \boldsymbol{\omega_B} - \boldsymbol{A_w}\, \widetilde{\dot{\boldsymbol{h}}_{\boldsymbol{w}}} \tag{12}$$

This is the control available from the RWs assembly and it is included in the close loop control of the CubeSat attitude. The continuous need of controlling the attitude of the satellite could lead to the saturation of the actuators if no actions are implemented. This is unwanted behaviour since a saturated actuator cannot provide anymore the control torque and need to be desaturated. The procedure implemented for the e.Cube tetrahedron assembly is reported in the following Section 4.4.2.

4.4.2 Continuous desaturation control of reaction wheels

The desaturation could be implemented in two different ways. One methodology consists of performing a desaturation manoeuvre with the thrusters after the RWs assembly is saturated. It requires the stop of the nominal mission mode to perform such manoeuvre. Another strategy is to continuously implement the desaturation during the nominal phase, to continuously control the status of the RWs. This second methodology is implemented for e.Cube.

The strategy implemented for e.Cube follows the findings obtained by Hogan and Schaub [17]. they proposed a methodology for the three-axis control using a redundant reaction wheels system with continuous momentum dumping. The desaturation strategy that they propose is based on magnetic dipole control to continuously maintain the reaction wheels below their operational limits. The methodology for the redundant system is implemented, to account for the four reaction wheels onboard the e.Cube satellite.

Starting from the wheel speed biases Ω_r, and a control gain c, the de-spin torque that needs to be applied on each reaction wheel is computed as

$$\boldsymbol{u_s} = -c\, \mathbf{J}_w\, (\boldsymbol{\Omega_w} - \boldsymbol{\Omega_r}) \tag{13}$$

The magneto torque bars can be used to provide a magnetic torque to counteract the wheels de-spin torque. The ideal magnetic dipole that should be commanded to the magnetic bars is computed as:

$$\boldsymbol{\mu_*} = -(\boldsymbol{B}\, \boldsymbol{G_t})^{\dagger}\, \boldsymbol{A_w}\, \boldsymbol{u_s} \tag{14}$$

where $\boldsymbol{B}$ is the Earth magnetic field vector, $\boldsymbol{G_t}$ is the matrix of torque bar alignment vectors, and $\boldsymbol{A_w}$ is the distribution matrix. Note that the superscript † is used to indicate the pseudoinverse matrix. Consequently, the resulting magnetic torque on the spacecraft is computed as

$$\boldsymbol{u_m} = -\boldsymbol{B}\, \boldsymbol{G_t}\, \boldsymbol{\mu_*} \tag{15}$$

An important consideration must be done, starting from the findings in [17]. It is rarely valid that the torque generated by the magnetic rods is equivalent to the necessary de-spin torque. For this reason, the unbalance motor torque is computed as

$$\boldsymbol{\Delta u} = \boldsymbol{A_w^{+}}\, (\boldsymbol{u_m} - \boldsymbol{u_s}) \tag{16}$$

with $\boldsymbol{A_w^{+}}$ the minimum norm inverse. This correction can be given by an attitude thruster module, to provide a correction torque on the spacecraft in the desaturation process. For CubeSat several cold gas thruster modules are already available on the market and can be used for attitude correction manoeuvres.

The unbalance motor torque can be provided by the on-off control of the thrusters. The thruster control is defined from the unbalance Δu as

$$\mathbf{u_t} = -\boldsymbol{\Delta u}\, \mathrm{sgn}(\boldsymbol{\omega_B}) \tag{17}$$

This control should be limited in rising time and fall time by a rate limiter, and is also subject to a delay time, sue to mechanical and electrical delays in valve circuits. This delay time is typical of about 5 msec, for most of the attitude thruster module available on the market.

5. Simulation Results

To demonstrate the feasibility of the control system for the e.Cube mission profile, some numerical simulation is implemented. As explained in Section 2 and 3, the re-entry phase with atmospheric data collection is simulated, since

it is the most demanding for the actuators. In fact, during this phase, the satellite flies on an elliptical orbit with the apogee at 550 km, and the perigee at 180 km. This results in a higher disturbance torque acting on the satellite at the pericentre, where the drag disturbance is more effective.

First, the ideal control is simulated, to provide an ideal command torque to the actuators, as presented in Section 5.1. Then, the commanded control is used as an input value to compute the actual control from the redundant reaction wheels system, where the tetrahedral configuration is employed. The results of this analysis are reported in Section 5.2. Finally, the inclusion of the desaturation in the close loop is implemented, considering both magneto torque and cold gas thrusters, as described in Section 5.3.

In this scenario, the goal is to re-orient the attitude of the spacecraft with the front face pointing the velocity direction. As described in Section 2, this requirement comes from the need of maintaining a three-axis stabilised configuration for a correct data collection of temperature and pressure load acting on the satellite during the passage in the upper atmosphere (below the altitude of 200 km). The spacecraft is assumed to have three magnetic bars oriented with the body frame, and four reaction wheels in tetrahedral configuration, as described in Section 4.4.1. Each reaction wheel has spin-axis inertia of about $J_{wi} = 2.34 \cdot 10^{-4}$ kg m^2. Moreover, the magnetic dipole is limited by the maximum dipole of the magneto torquers onboard, of about 1.19 Am^2. The parameters that were considered during the control loop are shown in Table 6, where the values for the control gains k_1 and k_2 are reported, together with the gain c for the desaturation and the matrix of torque bar alignment vectors G_t, equal to the identity matrix.

Table 6: parameters used for the numerical simulation.

Parameter	Value
$\boldsymbol{k_1}$	0.008
$\boldsymbol{k_2}$	0.0005
c	0.0005 s^{-1}
$\boldsymbol{G_t}$	$\boldsymbol{I_{3x3}}$

Moreover, in the simulation, the inertia matrix of the CubeSat is considered diagonal, and it was computed from the mass and geometry properties of the satellite. The e.Cube is a 12-unit satellite, with dimensions 30x20x20 cm, and a mass of about 15 kg. The principal moments of inertia are computed as follow:

$$I_{sat} = \begin{bmatrix} 0.1 & 0 & 0 \\ 0 & 0.16 & 0 \\ 0 & 0 & 0.16 \end{bmatrix} kg\ m^2 \tag{18}$$

Finally, at the initial condition, the satellite is assumed to be at the apocentre of the orbit described in Table 2. The initial angular velocity of the satellite in the body frame is assumed equal to $\omega_B = [1.25;\ -3.555;\ 3.07] \cdot 10\text{^} - 5$ rad/s. The numerical simulation propagates the attitude of the satellite for about 5 orbital periods.

The q-Metod for attitude reconstruction is applied in the simulation, considering the onboard sensors in Table 5. The determination error is of the order of 10^{-6} for the whole duration of the numerical simulation, as shown in Fig. 5. It provides an optimal least-square estimate of the attitude, more accurate than other methods, such as the TRIAD method [14], thanks to the information of sensor measurements vector in the body frame, to be compared with the same information in the inertial frame.

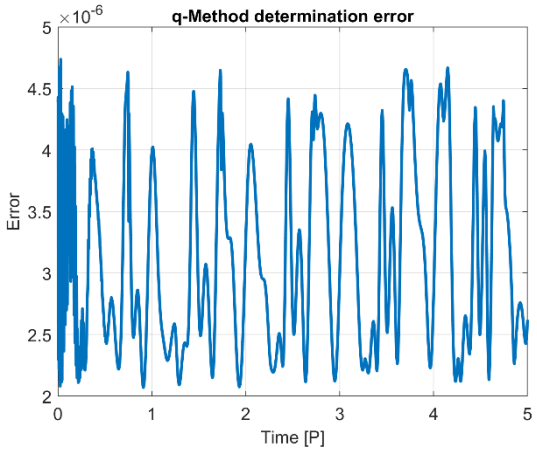

Fig. 5: q-Method determination error for the numerical simulation of e.Cube during the atmospheric data collection phase.

5.1 Ideal control

This section shows the results obtained in the numerical simulation, including the ideal control in the close loop. Fig. 6a represents the ideal control torque required to maintain the satellite with a velocity pointing attitude. The simulation lasts for five orbital periods and the ideal control requires about half of the orbital period to achieve the reference attitude profile. It can be observed that at the perigee passage, the control requires an additional effort to maintain the pointing attitude. This is due to the increased drag perturbation on the CubeSat, as it approaches the perigee.

In Fig. 6b the attitude errors are represented. On the top graph, the attitude matrix error is represented, as the trace of the difference between the unit matrix I and the attitude error matrix A_{BL}. This represents the difference among the body B and the reference attitude L. After less than half of the orbital period, the error tends asymptotically to zero. In the middle, the error on each component of the matrix is reported, where a small variation in the error behaviour is present at the perigee passage of the satellite, where the drag contribution is higher. Finally, on the bottom, the error on the angular velocity is represented, as the difference between the body and the reference angular velocity. As for the trace error, the angular velocity error tends to zero after half the orbital period.

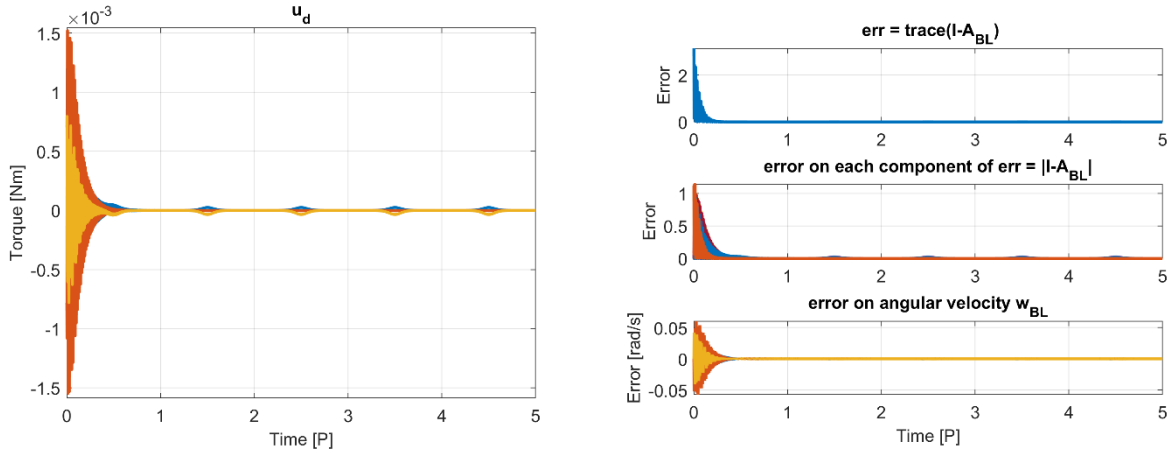

a. Ideal control torque **b. Pointing error to the reference attitude**

Fig. 6: Ideal control during the atmospheric data collection phase.

The tracking problem required the satellite to continuously follow the velocity vector. For this reason, the x and y components of the reference angular velocity are close to zero, to maintain the body frame aligned with radial and velocity direction. Moreover, the z component of the angular velocity is different from zero to allow continuous tracking of the velocity direction. Fig. 7 shows the body angular velocity (top graph) and the reference angular velocity (bottom graph). After an initial period to reach the convergence, the angular velocity of the body stabilises on the reference value, with x_b and y_b components around zero and the z_b component oscillating just above $1 \cdot 10^{-3}$ rad/s. The component in the z_b direction is the responsible for the velocity tracking of the CubeSat during the atmospheric data collection phase.

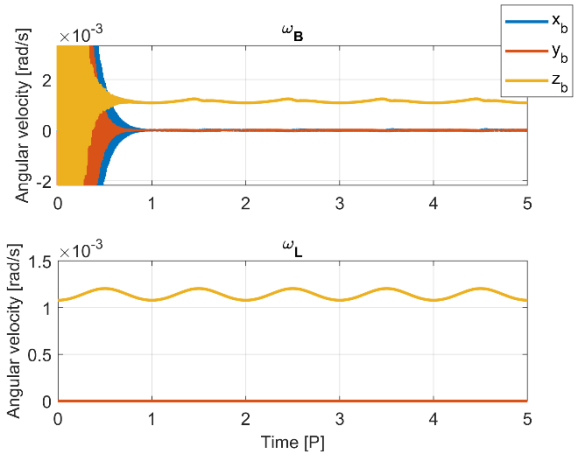

Fig. 7: Angular velocity of the satellite in the body frame (top figure) and reference velocity in the body frame (bottom figure)

5.2 Control with redundant reaction wheels

After the definition of the ideal control, the actuators are included in the close loop. At first, only the reaction wheels assembly is considered, without the desaturation contribution from magnetometers or thrusters. The ideal control act as the command control for the RWs assembly, which tries to follow the ideal behaviour for the tracking attitude. The results in terms of control torque and angular velocity tracking are shown in Fig. 8.

The tetrahedral configuration of the RWs manages to provide the reference tracking in less than half of the orbit period, as in Fig. 8a. Nevertheless, at about one orbital period there are some problems in the control effort. Looking at the angular velocity tracking in Fig. 8b, we saw that before one orbital period, the tracking is lost, and after that the body attitude became chaotic. This is caused by the saturation of the reaction wheels: the commanded control effort to maintain the tracking accumulates in time and lead to the saturation of the angular momentum $\boldsymbol{h_w}$.

This behaviour is unwanted and requires a further implementation of the control law, with the inclusion of other actuators to compensate for this problem.

When a reaction wheel saturates, an external momentum should be applied to the system to reduce the angular momentum of the wheel to the desired bias value. For a non-redundant system, with three RWs, to compensate the saturation, a momentum proportional to the difference between the actual momentum and the desired bias can be applied. This simple correction drives the wheel speed toward a desired reference value.

Nevertheless, for a redundant system, as the case of the e.Cube, a four-RWs assembly has an infinite number of wheel speed that drives toward the desired value. For this reason, a different control is used in the numerical simulation, as described in Section 4.2.2, from [17]. The control law introduced by Hogan and Schaub could help the system to reduce the required torque, even if it results in a long time for convergence. The numerical results including the continuous desaturation moment are described in Section 5.3.

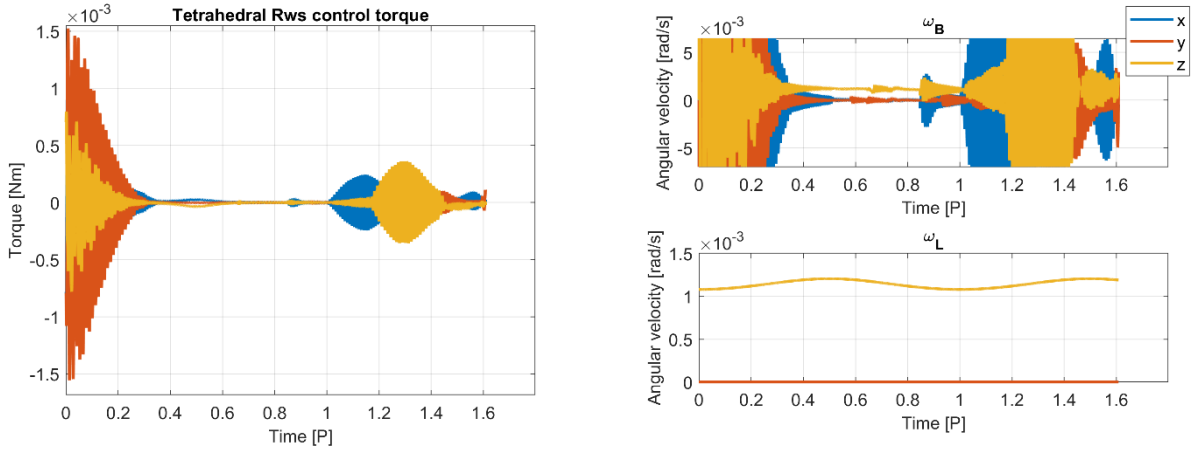

a. RWs control torque **b. Angular velocity in the body frame**

Fig. 8: Control with tetrahedral RWs assembly, with the control torque on the left, and the angular velocity on the right.

5.3 Control with redundant reaction wheels and continuous desaturation

As described in Section 5.2, the system needs the implementation of a desaturation law to deal with the high disturbance torque acting on the satellites and reduce the effort on the reaction wheels assembly. During the atmospheric data collection phase, the drag torque increases around the perigee position and requires an additional control effort to maintain the attitude. The torque caused by the drag is represented in Fig. 9, where it can be observed the substantial increase in the torque value at each perigee passage.

In Fig. 10 is represented the control of the e.Cube mission when the magneto torquers are used to provide a continuous contribution to the desaturation of the wheels. From the control effort, in Fig. 10a, the satellites manage to follow the ideal control low much longer than in the previous case, without the continuous desaturation. In the case described in Section 5.2 the control was maintained less than one orbital period, while in this case under analysis, the satellite maintains the tracking of the reference trajectory for more than two orbital periods. This behaviour translates in the tracking of the angular velocity, as in Fig. 10b, where the comparison between the body and the reference angular velocity is shown.

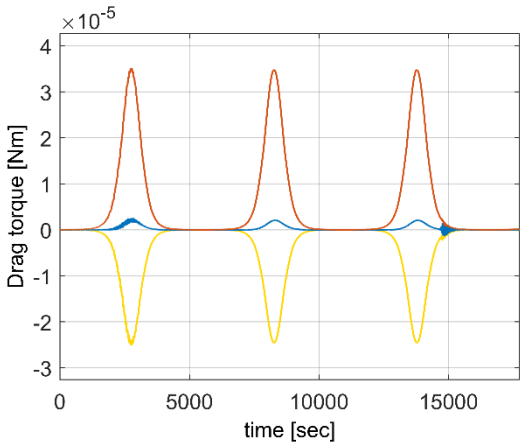

Fig. 9: Drag torque on the e.Cube spacecraft during the atmospheric data collection phase.

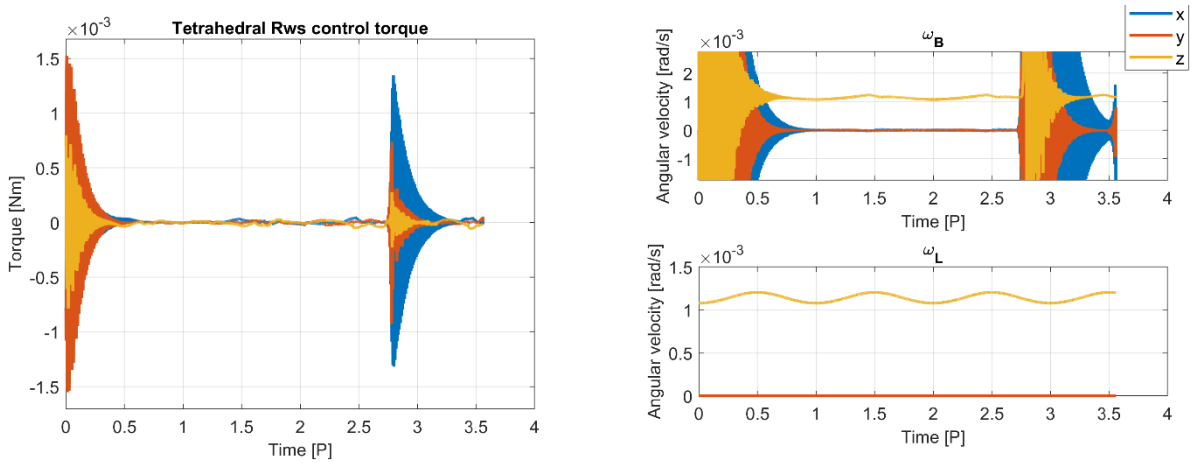

a. RWs control torque **b. Angular velocity in the body frame**

Fig. 10: Control with tetrahedral RWs assembly, including the desaturation effort with the magnetorquers, with the control torque on the left, and the angular velocity on the right.

Even if the numerical results that are shown in Fig. 10 improve the situation described in Section 5.2, it does not solve completely the saturation problem. As explained in [17], the magnetic torquer is not able to provide an exact compensation torque to the satellite: $u_{magn} \neq u_{W_{desaturation}}$ in general.

For this reason, the need of including a cold gas assembly to monitor the behaviour of the control moment is favoured. The thrusters should provide an additional control moment to balance the difference between the desaturation torque and the compensation torque. This control, as described in Section is superimposed to the RWs control torque and provide a net-zero torque on the spacecraft, resulting in the desaturation torque.

6. Conclusions

In this paper, a preliminary attitude dynamics and control system design is developed for the e.Cube mission concept. Specifically, the control law is implemented in a close loop to account for external disturbance torque, which is essential to describe the attitude behaviour of the satellite. A feedback control law is implemented considering a redundant reaction wheel assembly, in tetrahedral configuration, together with the contribution of the magnetic torquers for a desaturation effect. The numerical analysis focuses on the atmospheric data collection phase of the e.Cube mission. This phase was of particular interest, due to the high level of disturbance torque due to the atmospheric drag. Moreover, to provide a correct measurement environment for the temperature and pressure sensors, the velocity tracking frame is considered in the numerical simulations.

The results of the analyses show the need of including in the ADCS system a cold gas module to supervise the desaturation control law of the magnetic rods. Future work will be to implement in the close loop the cold gas thruster to provide continuous tracking of the reference attitude for the e.Cube mission. This is of primary importance to provide a continuous measurement of the physical properties of the upper atmosphere, below 200 km of altitude. As described in Section 1, the characterisation of the thermosphere load on the satellite during the re-entry phase could highly increase the accuracy of the re-entry prediction and provide a more accurate model of the thermosphere density. The e.Cube mission is envisioned to improve the current knowledge of atmospheric physical properties to help and improve the design of future space mission.

Acknowledgements

The work presented in this paper was funded by the European Research Council (ERC) under the European Unions Horizon 2020 research and innovation program (grant agreement No. 679086 COMPASS).

The authors acknowledge the scientific and tecnological partners of the e.Cube project, Stefano Antonetti, Francesco Di Tolle, Roberto Redaelli and Francesco Lisi from D-Orbit, Luca Marrocchi, Marco Alberti from TEMIS, Alessandro Francesconi and Lorenzo Olivieri from Univerità di Padova and Massimo Tipaldi from Intelligentia.

References

[1] Colombo, Camilla; Trisolini, Mirko; Scala, Francesca; Brenna, Marco Paolo; Gonzalo, Juan Luis; Antonetti, Stefano; Di Tolle, Francesco; Redaelli, Roberto; Lisi, Francesco; Marrocchi, Luca; Alberti, Marco; Francesconi, Alessandro; Olivieri, Lorenzo; Tipaldi, Massimo. e.Cube mission: the environmental CubeSat. *8th European Conference on Space Debris.* ESA/ESOC, Darmstadt, Germany. 2021, April 20-23 (In press).

[2] Kuang D., et al. "Measuring atmospheric density using GPS–LEO tracking data." *Advances in Space Research* 53.2 (2014): 243-256.

[3] Trisolini M., Lewis H.G., Colombo C., Spacecraft design optimisation for demise and survivability, Aerospace Science and Technology, 2018, Vol. 77, pp. 638-657, DOI: 10.1016/j.ast.2018.04.006

[4] Trisolini M., Lewis H.G., Colombo C., Demisability and survivability sensitivity to design-for-demise techniques, Acta Astronautica, April 2018, 10.1016/j.actaastro.2018.01.050

[5] Trisolini M., Lewis H. G., Colombo C., Constrained optimisation of preliminary spacecraft configurations under the design-for-demise paradigm, *Journal of Space Safety Engineering*, 2021, In press, DOI: 10.1016/j.jsse.2021.01.005

[6] De Pasquale E., et al. "ATV Jules Verne reentry observation: Mission design and trajectory analysis." *2009 IEEE Aerospace conference*, IEEE, 2009.

[7] Grinstead J., et al. "Airborne observation of the Hayabusa sample return capsule re-entry." *42nd AIAA Thermophysics Conference*, 2011.

[8] Ailor W., et al. "REBR: An Innovative, Cost-Effective System for Return of Reentry Data." *AIAA SPACE 2007 Conference & Exposition*, 2007.

[9] Miccoli C., "Detailed Modeling of Cork-Phenolic Ablators in Preparation to the Post-Flight Analysis of the QARMAN Re-Entry CubeSat", Diss. Politecnico di Torino, 2020.

[10] Hyperion technologies, https://hyperiontechnologies.nl/, last visited 10/04/2021.

[11] NewSpace Systems, https://www.newspacesystems.com/portfolio/magnetorquer-rod/, last visited 10/04/2021.

[12] Microspace srl, http://www.microspace.it/, last visited 10/04/2021.

[13] GOM space, https://gomspace.com/home.aspx, last visited 10/04/2021.

[14] OCE Technology, http://ocetechnology.com/, last visited 10/04/2021.

[15] Markley, F. Landis. "Attitude determination using vector observations and the singular value decomposition." *Journal of the Astronautical Sciences* 36.3: 245-258, 1988.

[16] Premerlani, W., & Bizard, P. Direction cosine matrix imu: Theory. *Diy Drone: Usa*, 13-15, 2009.

[17] Bar-Itzhack, I. Y., & Harman, R. R. Optimized TRIAD algorithm for attitude determination. *Journal of guidance, control, and dynamics*, *20*(1), 208-211, 1997.

[18] Hughes, Peter C. *Spacecraft attitude dynamics*. Courier Corporation, 2012.

[19] Kök, Ibrahim. Comparison and analysis of attitude control systems of a satellite using reaction wheel actuators. 2012.

[20] Hogan, Erik A.; Schaub, Hanspeter. Three-axis attitude control using redundant reaction wheels with continuous momentum dumping. *Journal of Guidance, Control, and Dynamics*, 2015, 38.10: 1865-1871.